

Enhancement of Corrosion Resistance of Mild Steel Plate Using Zn/Ti Nanocomposite for Industrial Applications

N. Guruprasath¹, S. Surendhiran¹, V. Gowtham², M. Vijayaprakash¹, PR. Senthilmurugan¹

¹Centre for Nano Science and Technology, K. S. Rangasamy College of Technology, Tiruchengode, Tamil Nadu, India

²Centre for Nano Science and Technology, Pondicherry University, Pondicherry, India

ABSTRACT

Zinc/ Titania nanocomposite prepared by Sonication assisted Solid state reaction method. The prepared Zn/Ti nanocomposite has been employed to improve the corrosion resistance behavior of Mild Steels (MS) which are mostly used in sugarcane and paper making industries. The physiochemical characteristics of the prepared Zn/Ti nanocomposite were evaluated by various characterization techniques such as X-ray diffraction (XRD), Fourier Transform Infrared Spectroscopy (FTIR), Scanning electron microscopy (SEM), X-ray fluorescence spectroscopy (XRF) and so on. The improvement of corrosion resistance of mild steel plate has been evaluated by Linear Sweep Voltammetry (LSV). As from the obtained results, Corrosion resistance behavior of MS has been improved 85% by the prepared Zn/Ti nanocomposite coating on it. Thus the prepared Zn/Ti nanocomposite could be a potential candidate as corrosion inhibitor in various industries.

Keywords : Zn/Ti nanocomposite, Linear Sweep Voltammetry, Improved Corrosion Inhibition.

I. INTRODUCTION

Mild steel is a valuable construction material used in countless industries mostly for its finest mechanical properties and its almost cost effective compared to other materials. Sugar and paper industries are the vital part of the world economy. In sugar and paper industry most of the equipment parts were made out of mild steel (MS). Hence it is used as construction material of machinery and equipment in sugar industry. However, it has poor corrosion resistance in that environmental condition. Sugar and paper industries are plagued by high maintenance, replacement and repair of equipment due to corrosion and abrasion. There are two possible ways to improve the corrosion, one is coating of nanomaterials on

needed metal surface and another one is alloying. Over the past decade large number of nanomaterials such as Al₂O₃, NiO, and ZnO etc., has been studied corrosion inhibitor for different metal plates under aqueous, acid solution and environmental conditions. The role of corrosion inhibitor is the prevention of the adsorption of violent anions and reduction of the peeling rate of the passivation oxide during the analysis and environmental atmospheres.

Among these materials, ZnO nanostructures have been widely studied, as they are high in corrosion resistance and surface properties. Numerous nanocomposite and its incorporation with natural and synthetic polymers have been studied as corrosion protection materials in the past. Nanocomposites of

Zn/Ti find a comprehensive applications in photo and electro catalysis, energy conversion and storage devices etc. However, a detailed survey on literature suggests that anticorrosion study of Zn/Ti nanocomposite has been hardly attempted. Nanomaterials have been coated by a variety of techniques namely dip coating, spray pyrolysis, and spin coating and doctor's plate method. Among them, doctor's blade method is considered to be an economical simplest and fastest method for coating materials for various applications.

In this research work, we represent about the preparation of Zn/Ti nanocomposite by Sonication assisted solid state reaction method. The prepared Zn/Ti nanocomposite has been employed for anticorrosive properties of mild steel for industrial applications. The structural, morphological and physiochemical properties of Zn/Ti nanocomposite has been studied elaborately.

II. EXPERIMENTAL DETAILS

2.1 Materials

Zinc oxide (ZnO: Merck), Titanium dioxide (TiO₂: Merck), Mild steel (MS) are used to prepare Zn/Ti nanocomposites, sugarcane juice, Sodium Hydroxide (NaOH) were used to prepare the electrolytes

2.2 Method

Zn/Ti nanocomposites were prepared by sonication assisted Solid state reaction method. Three different ratio Zn/Ti nanocomposites were prepared to study a comparative analysis on structural, morphological and anticorrosive behavior of MS plate. The weight ratio of 1:2, 2:2 and 2:1 g of ZnO and TiO₂ powders were taken to prepare the Zn/Ti nanocomposite. One grams of ZnO and Two grams of TiO₂ were dissolved in 100ml of ethanol and stirred for 5 min to get homogenous solutions. Afterwards, the ethanol solution was transferred to Sonicator and sonicated for 30 min with 40 Hz. Then, the Sonicated solution was dried in hot plate at 80 °C for 3 hours which is

further calcination at 600 °C for 3 hours using muffle furnace. The obtained powder is further grinded finely using mortar pestle. Hereafter, 1:2 g weight ratio of ZnO and TiO₂ sample named as Zn/Ti 1 and Zn/Ti 2, Zn/Ti 3 named respectively for 2:2 and 2:1 g of ZnO and TiO₂ samples. The graphical representation of the preparation procedure is shown in figure 1.

2.3 Sample preparation for corrosion studies

MS plate was exploited to study the anticorrosive behavior of Zn/Ti nanocomposite. The mild steel subsequently polished with 1mm SiC grit paper which is cleaned with acetone. The prepared Zn/Ti nanocomposite of 1 mg was mixed with small pinch of polyvinylidene fluoride (PVDF) (0.15 mg) and one drop of N-methyl-2-pyrrolidone (NMP) at 80:15:5 weight ratios in order to get the slurry state. The prepared slurry state was coated over on the surface of the MS plate using doctor's blade technique. The coated plate was dried for 1 h in an oven at 60 °C and then used for linear sweep voltammetry (LSV) and electrochemical impedance spectroscopy (EIS) under two electrolyte namely raw sugarcane extract and pH adjusted sugar cane extract (7 pH). The MS plate and prepared Zn/Ti nanocomposite coated MS plates are shown in figure 2.

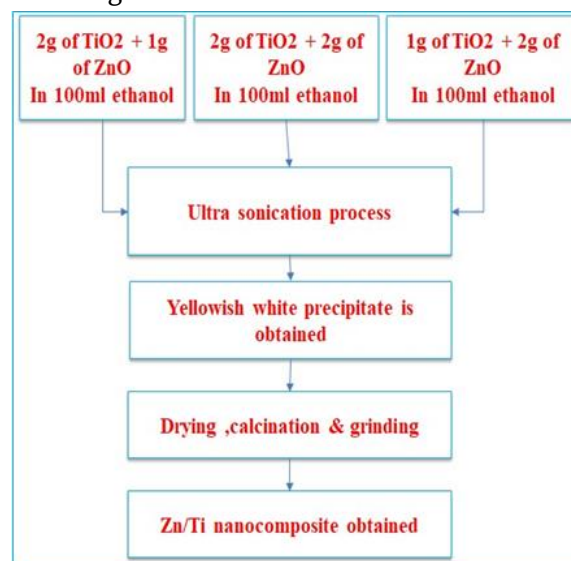


Fig.1 The graphical representation of the preparation procedure

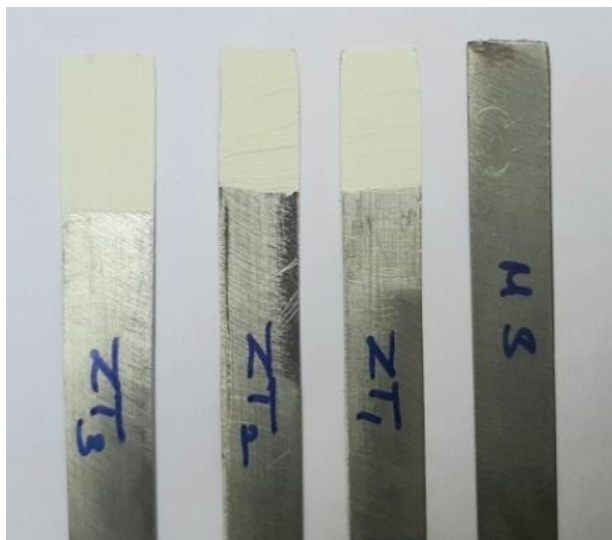


Fig. 2. Uncoated and Zn/Ti nanocomposite coated MS plates

III. RESULTS AND DISCUSSION

3.1 X-ray Diffraction pattern

The XRD spectra of Zn/Ti nanocomposite is shown in figure 3. The observed XRD pattern of the prepared material reveals the presence of crystalline nature. The XRD patterns contain both diffraction peaks of ZnO and TiO₂. The XRD patterns are highly matched with standard JCPDS and earlier reports. The reference pattern 98-002-8861 shows the ZnO has hexagonal phase while the reference pattern 98-000-5226 shows the TiO₂ has tetragonal phase. The diffraction peaks at ZT1, ZT2 & ZT3 are indexed with their corresponding hkl values for ZT1, ZT2 & ZT3 respectively, and hence Zn / Ti samples have shift in both phases with the increase in composition of ZnO and TiO₂. Also the peak broadening describes the smaller crystallite size of the prepared Zn/Ti nanocomposite. The XRD diffraction peak intensities for the prepared materials are varied due to the ratios taken but there is no additional peaks observed for any samples. The observed result shows that the average crystal size of the Zn/Ti composite is 15.877, 12.145 and 14.33 respectively for ZT1, ZT2 and ZT3 is obtained by using form Debye Scherrer equation. As

we concluded from the obtained result the equal ratio (ZT2) nanocomposite shows better crystallinity and high purity and low crystalline size compared with other two nanocomposites.

3.2 Fourier Transform Infrared spectroscopy

The FTIR spectra for Zn/Ti composite were analysed in the range of 400 to 4000 cm⁻¹. The Figure 4 shows the FTIR spectra of the prepared Zn/Ti nanocomposites. FT-IR spectra of ZT1, ZT2 & ZT3 shows more likely similar absorption peaks at 566, 792, 1385, 1632, 1742, 2928 and 3433cm⁻¹. From Fig.4 the band observed at 566 cm⁻¹ for stretching vibration of Zn and Ti-O band peak at 466 cm⁻¹. The weak band near 1,632 cm⁻¹ is assigned to H-O-H bending vibration mode due to the adsorption of moisture when FT-IR sample disks were prepared in an open air atmosphere. The wide band at 3433 cm⁻¹ is corresponding to the presence of hydroxyl groups (-OH).

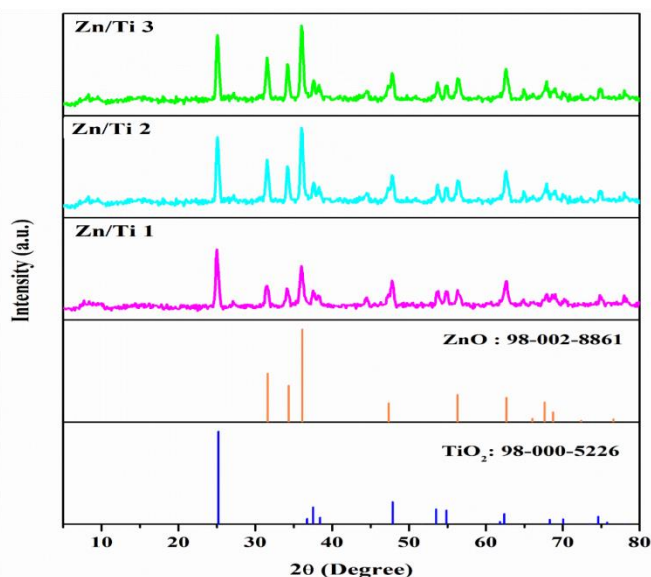


Fig. 3. XRD pattern of Zn/Ti nanocomposites

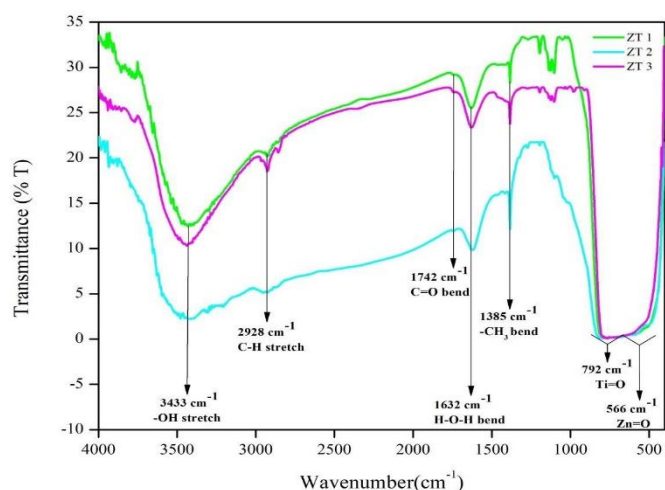


Fig.4. FTIR Spectra of Zn/Ti nanocomposites

3.3 UV-Vis Spectroscopy

UV-Vis spectra of Zn/Ti nanocomposite is shown in Fig.5 The observed UV adsorption peaks are raised at 397, 392 and 387 nm for ZT1, ZT2 & ZT3 nanocomposites respectively. The adsorption peaks shows red shift while comparing with early reports of ZnO and TiO₂. ZT2 shows higher adsorption behavior due to its lower crystalline size and excellent purity compared with other two nanocomposites. According to quantum confinement effect, the UV-visible adsorption spectra intensity clearly depends on the crystalline size of Zn/Ti nanocomposite. The band gap energy values of the prepared nanocomposite were calculated by Tauc relations. The calculated band gap values are given in table 1 and the relation between crystalline size, absorbance wavelength and band gap are compared in table 1.

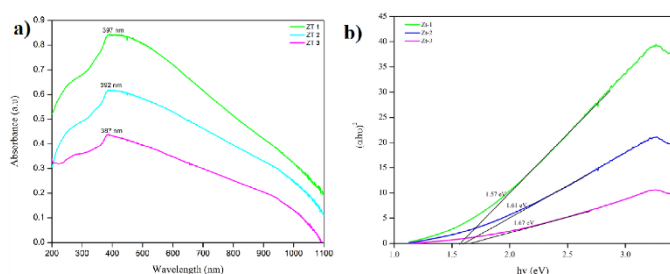


Fig. 5 a) UV-Vis spectra, **b)** Tauc plot of Zn/Ti nanocomposite

Table 1. The relation between crystalline size, absorbance wavelength and band gap

| Nanocomposite | Crystalline size from XRD (nm) | Absorbance wavelength (nm) | Bandgap (eV) |
|---------------|--------------------------------|----------------------------|--------------|
| ZT 1 | 18.606 | 397 | 1.57 |
| ZT 2 | 15.877 | 392 | 1.61 |
| ZT 3 | 17.250 | 387 | 1.67 |

3.4 X-ray Fluorescence Spectroscopy

Table 2 and 3 shows the elemental composition of the prepared Zn/Ti nanocomposite and MS plate which was used in this work to evaluate the electrochemical behaviors of Zn/Ti nanocomposite. The results show the purity level of the prepared material which supports the results already discussed (XRD, FTIR and UV-Vis). The elemental composition are varied for the ratio taken to prepare Zn/Ti nanocomposite.

Table 2. Elemental analysis of Zn/Ti nanocomposite

| Sample | Analytes | | Total |
|--------|------------------|--------|-------|
| | TiO ₂ | ZnO | |
| ZT1 | 70.66% | 29.33% | 100 % |
| ZT2 | 59.32% | 40.67% | 100 % |
| ZT3 | 26.81% | 73.19% | 100 % |

Table 3. Elemental analysis of MS plate

| Samples | Analytes | Result | Line |
|--------------|----------|--------------|------|
| MS Plate | Fe | 82.430 | Feka |
| | Cr | 17.350 | Crka |
| | Ni | 0.122 | Nika |
| | Cu | 0.097 | Cuka |
| Total | | 100 % | |

3.5 Surface morphological images

Figure 6a, b, and c shows the SEM images of the ZT1, ZT2 and ZT3 nanocomposites respectively. From these images, it is observed that spherical shaped ZT nanocomposites are embedded with each other's. The uniform distributions of the particle could be seen in the SEM images it may be happened due the ultrasonic wave's irradiation process during the synthesis of ZT nanocomposites. The spherical structure of ZT nanocomposites offers additional electron transport from the electrode/electrolyte interface due to the high surface to volume ratio of spherical structures compared to other nanostructures during the electrochemical studies.

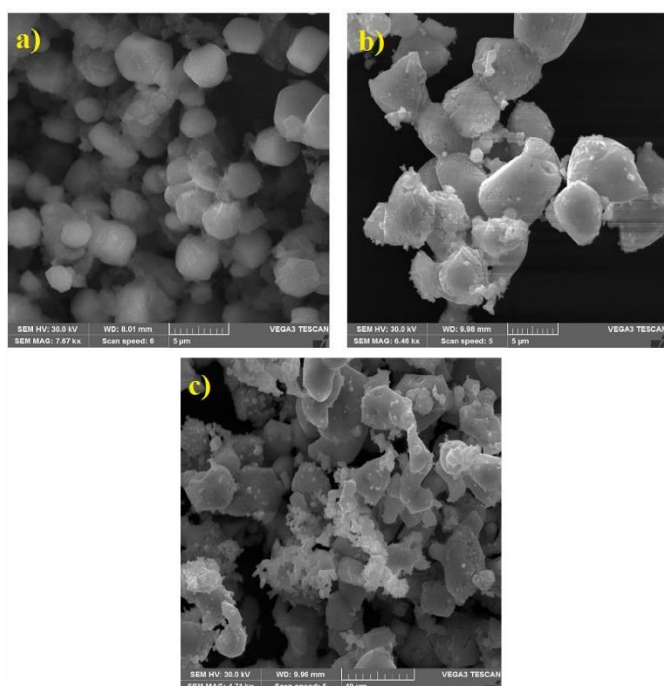


Fig 6. SEM images of Zn/Ti nanocomposites

The figure 7 shows the optical images of the surface of the uncoated and ZT nanocomposites coated MS plates. These optical surface images were captured from 40X lens microscope. The images are clearly shows the surface scratches of the MS plate for before and after the coating. The ZT nanocomposites coating on MS plate shows the decreased surface roughness of plates.

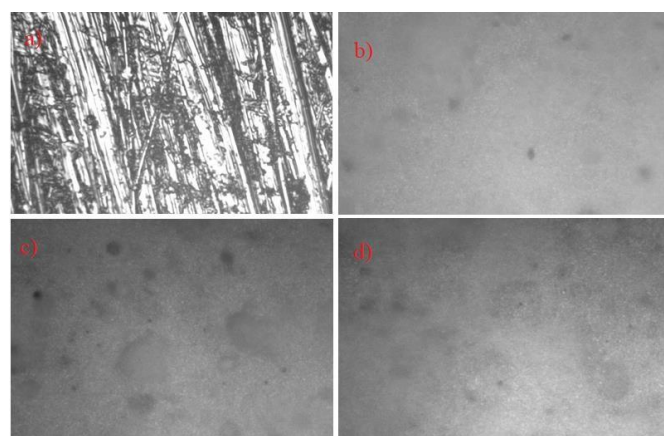


Fig. 7. Optical images of uncoated (a) and ZT1 (b), ZT2 (c) and ZT3 (d) coated MS plates 3.6 Electrochemical Corrosion Studies

Figure 8 shows the Tafel plots of uncoated and ZT nanocomposites coated MS plates in raw sugarcane juice and pH adjusted sugarcane juice (pH ~ 7.0). The comparative corrosion studies are individually carried out for MS plate and ZT nanocomposite coated MS plates (MS/ZT) samples. Initially, the potential is applied at 1.4 V and the corrosion initiated at MS plate anode and its potential tends to move for 0 V with constant interval of 0.5 m/V. It is observed that corrosion potential of all MS/ZT plates is shifted toward positive side (anodic region) compared to uncoated MS plate.

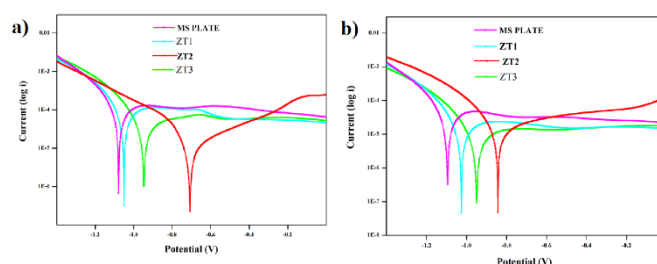


Fig. 8. Tafel plots of the prepared Zn/Ti nanocomposites under two electrolyte mediums

It was also obvious that the MS/ZT has lower corrosion current compared to MS plate suggests improve corrosion resistance achieved due to ZT nanocomposite coating over MS plate surface. The above results assured that low corrosion rate and high

electrochemical corrosion resistance is achieved by a thin layer coating of ZT nanocomposite over the anode surface where MS acts. For the raw sugarcane juice, the improved corrosion resistance is observed for ZT 2 and ZT 3 and they are 75.55 and 48.42 % compared with uncoated MS plate. Interestingly, the improved corrosion resistance for ZT2 plate under pH adjusted sugarcane juice is 96.59 % which nearly two time higher than other plates. The calculated potentiodynamic polarization parameters are tabulated in table 4.

Table 4. Potentiodynamic polarization parameters of uncoated and Zn/Ti nanocomposites coated MS plates under two electrolytes

| Electrolyte | Sampl es | Ecorr (mV) | I _{corr} (A/Cm ²) | Corrosi on Rate (mm/yr) | Polarizati on Resistanc e (Ω) | IE % |
|-----------------------------|----------|------------|--|-------------------------|-------------------------------|------|
| Raw Sugarcane juice | MS Plate | 945.61 | 18.136 | 0.21074 | 1.19790 | - |
| | ZT1 | 715.56 | 14.389 | 0.1672 | 3.78820 | 20.6 |
| | ZT2 | 1.0512 | 5.1588 | 0.05994 | 781.570 | 71.5 |
| | ZT3 | 1.0788 | 5.3267 | 0.10896 | 628.890 | 48.4 |
| pH adjusted Sugarcane juice | MS Plate | 1.0281 | 38.029 | 0.44189 | 899.720 | - |
| | ZT1 | 949.66 | 31.890 | 0.27056 | 1.59040 | 38.5 |
| | ZT2 | 845.83 | 1.2935 | 0.01503 | 4.50406 | 96.5 |
| | ZT3 | 1.0953 | 182.18 | 0.21169 | 463.680 | 52.0 |

IV. CONCLUSION

Zn and Ti based nanocomposites have been successfully synthesized using ultrasonic waves assisted solid state reaction method. The structural investigation of the sample is analyzed by XRD which clearly specifies that the prepared sample is mixed

phase with cubic and tetragonal structure with crystallite sizes ranges from 18.5 to 12 nm. The spherical shaped ZT nanocomposites have been evidently observed from SEM micrographs. The size computed from SEM images is well coordinated with XRD patterns. The corrosion studies under raw and pH adjusted sugarcane juices have been analyzed in terms of coated on MS plate. As from the obtained results, Corrosion resistance behavior of MS has been improved by ZT 2 nanocomposite coating for 71.55 and 96.59 % respectively for raw and pH adjusted sugarcane juices. In general, the attained results are finely supported to show the prepared ZT nanocomposites by ultrasonic waves assisted solid state method are promising candidates for anticorrosive applications of MS steel for industrial ranges.

V. REFERENCES

- [1]. Kalpana Vajpayee, Ashutosh Bajpai, (2021), Corrosion resistance & Its Impact on Sugar Quality in Cane Sugar Industry IJERT. Vol.10 Issue 02, PAPER ID: IJERTV10IS020244
- [2]. K. C. Suresh & A. Balamurugan (2020), Evaluation of structural, optical, and morphological properties of nickel oxide nanoparticles for multi-functional applications, Inorganic and Nano-Metal Chemistry, ISSN: 2470-1556, DOI:10.1080/24701556.2020.1770793
- [3]. Da Chen, Hao Zhang, Song Hu and Jinghong Li, (2007), Preparation and Enhanced Photoelectrochemical Performance of Coupled Bicomponent ZnO-TiO₂ Nanocomposites. American Chemical Society, Vol. 112, No. 1, DOI: 10.1021/jp077236a
- [4]. Azadeh Haghhighatzadeh, Mahsa Hosseini, Babak Mazinani and Mohammadreza Shokouhimeh, (2019) Improved photo catalytic activity of ZnO-TiO₂ nanocomposite

- catalysts by modulating TiO₂ thickness, *Mater. Res. Express*, DOI: 10.1088/2053-1591/ab49c4
- [5]. Camila A. Farias Vanessa F. C, Belo Horizonte, Minas Gerais, (2011), Corrosion resistance Resistance of Steels Used in Alcohol and Sugar Industry, *Chem. Eng. Technol.* 34, No. 9, 1393–1401, DOI: 10.1002/ceat.201000542
- [6]. Aslam, J.; Mobin, M.; Aslam, R.; Ansar, F, (2020), corrosion resistance protection of low carbon steel by conducting terpolymer nanocomposite coating in 3.5 wt% NaCl solution. *J. Adhes. Sci. Technol*, Vol. 34, Issue 4, DOI: 10.1080/01694243.2019.1676599
- [7]. Cooke, K.O.; Khan, T.I, (2018), Effect of thermal processing on the tribology of nanocrystalline Ni/TiO₂ coatings. *Emerg. Mater*, DOI: 10.1007/s42247-018-0015-z
- [8]. Kallappa, D.; Venkatarangiah, V.T, (2020) Synthesis of CeO₂ doped ZnO nanoparticles and their application in Zn-composite coating on mild steel. *Arab. J. Chem*, Vol.13, Issue 1, 2309-2317, DOI: 10.1016/j.arabj.2018.04.014
- [9]. Vichuda Lachom, Phitsanu Poolcharuansin and Paveena Laokul, (2017), Preparation, Characterizations and Photocatalytic Activity of a ZnO/TiO₂ Nanocomposite, *Mater. Res. Express*, DOI: 10.1088/2053-1591/aa60d1
- [10]. mprakash Sahu , (2018), Assessment of sugarcane industry: Suitability for production, consumption, and utilization. *Annals of Agrarian Science*, 389–395, DOI:10.1016/j.aasci.2018.08.001
- [11]. Dr. Rathika.govindasamy , swetha ayappan, (2015), study of corrosion inhibition properties of novel semicarbazones on mild steel in acidic solutions. *J. Chil. Chem. Soc.*, 60, 2015, DOI: 10.4067/S0717-97072015000100004
- [12]. Chuan Lai a,b , Bin Xie b,† , Like Zou b , Xingwen Zheng b , Xiao Ma b , Shasha Zhu b, (2017), Adsorption and corrosion inhibition of mild steel in hydrochloric acid solution by S-allyl-O,O0 –dialkyldithiophosphates, *Results in Physics* 7, 3434–3443 DOI:10.1016/j.rinp.2017.09.012
- [13]. Mitra Gholami, Mehdi Shirzad-Siboni, Mahdi Farzadkia & Jae-Kyu Yang, (2016) Synthesis, characterization, and application of ZnO/TiO₂ nanocomposite for photocatalysis of a herbicide (Bentazon), *Desalination and Water Treatment*, 13632-13644, DOI: 10.1080/19443994.2015.1060541
- [14]. G. Nagarajua, *, Udayabhannua , Shivaraja , S.A. Prashanthb , M. Shastric , K.V. Yathisha , C. Anupamad , D. Rangappac, (2017), Electrochemical heavy metal detection, photocatalytic, photoluminescence, biodiesel production and antibacterial activities of Ag–ZnO nanomaterial, *Materials Research Bulletin*, 54–63, DOI:10.1016/j.materresbull.2017.05.043 0025-5408
- [15]. Dongfeng Shao, Qufu Wei , (2018), Microwave-Assisted Rapid Preparation of Nano-ZnO/Ag Composite Functionalized Polyester Nonwoven Membrane for Improving Its UV Shielding and Antibacterial Properties, *Materials*, 1412, DOI:10.3390/ma11081412
- [16]. Cláudia G. Silvaa,, Maria J. Sampaioa, Rita R.N. Marques , Liliana A. Ferreiraa, Pedro B. Tavares , Adrián M.T. Silvaa, Joaquim L. Faria, (2015), Photocatalytic production of hydrogen from methanol and saccharides using carbon nanotube-TiO₂ catalysts, *Applied Catalysis B Environmental*, DOI: 10.1016/j.apcatb.2014.10.032